J Appl Electrochem (2009) 39:233–240
DOI 10.1007/s10800-008-9661-9

ORIGINAL PAPER

Modulation of magnetic and structural properties of cobalt thin films by means of electrodeposition

Jose García-Torres · Elvira Gómez · Elisa Vallés

Received: 28 March 2008 / Accepted: 3 September 2008 / Published online: 23 September 2008

Abstract Cobalt electrodeposits were prepared from an electrolytic bath containing cobalt perchlorate. The effect of different species, organic (thiourea and sodium gluconate) and inorganic (boric acid), on the crystallographic structure, morphology, magnetic properties and electrochemical behaviour of cobalt electrodeposits was investigated. Amorphous cobalt, hcp cobalt and a non-usual primitive cubic cobalt phase were observed depending on the bath composition. Depending on the structure, different morphologies and magnetic properties were found. Coercivity values of the cobalt coatings ranged from around 15 Oe for amorphous, nodular deposits to 380 Oe for cobalt coatings showing acicular morphology and hcp structure with a (002) preferred orientation. Knowledge of the influence of the species on the properties of cobalt makes it possible to obtain tailored cobalt films.

Keywords Cobalt coatings · Electrodeposition · Magnetic properties · Crystal structure

1 Introduction

Electrodeposition is an efficient tool for preparing films for new technological applications. This method is cheaper in terms of equipment and less time consuming than other available deposition techniques. One of the metals successfully deposited by this method is cobalt. The electrodeposition of cobalt metallic layers and alloys is of considerable interest due to its potential applications in several fields [1, 2], especially in microelectronics for magnetic recording systems [3, 4]. Cobalt is one of the most important ferromagnetic components of magnetic thin film materials. Electrodeposition is also of interest for the preparation of cobalt and cobalt alloys because it makes it possible to modulate the structure of deposits and, hence, their magnetic properties. Depending on the preparation conditions, i.e. electrolyte composition, temperature, applied potential and presence of additives, materials with different structures, morphologies and magnetic properties can be obtained. The effects of bath compositions as well as the influence of solution parameters (pH, temperature) and electrodeposition conditions have been reported [5–7].

Our research is focused on the electrolytic preparation of cobalt based materials, one of our objectives being the preparation of nanostructured heterogeneous Co–Ag deposits. The electrolytic bath developed for this purpose contains various species: thiourea, sodium gluconate and boric acid [8, 9]. Given that the constituents of the electrolytic bath influence the deposit properties, the objective of the present study is to determine the effect of each one of the non-electroactive species present in the Co–Ag bath on the properties of pure-cobalt electrodeposits. The study focuses not only on the influence of each non-electroactive species and their combinations on deposits characteristics but also on establishing the relationship between the morphology, structure and magnetic properties of cobalt films prepared from the different electrolytic baths. This study seeks to obtain background information about the effect of each species present in the bath on the cobalt coatings and hence to facilitate the preparation of Co–Ag deposits with tailored properties.

J. García-Torres · E. Gómez · E. Vallés (✉)
Electrodep, Departament de Química Física and Institut de Nanociència i Nanotecnologia (IN 2 UB), Universitat de Barcelona, Martí i Franquès 1, 08028 Barcelona, Spain
e-mail: e.valles@ub.edu

2 Experimental section

Electrodeposition of cobalt coatings was performed from different baths summarized in Table 1. Chemicals used were $Co(ClO_4)_2$, CSN_2H_4 (thiourea), H_3BO_3, $C_6H_{11}NaO_7$ (sodium gluconate) and $NaClO_4$, all of analytical grade. All solutions were freshly prepared with water treated with a Millipore Milli Q system, de-aerated with argon and maintained under argon atmosphere during the electrochemical experiments. The pH of the bath selected for electrodeposition was maintained at 3.7. In all cases temperature was kept constant at 25 °C.

Electrodeposition was performed in a conventional three-electrode cell using a microcomputer-controlled potentiostat/galvanostat Autolab with PGSTAT30 equipment and GPES software. Cobalt films were deposited on vitreous carbon substrates. In order to avoid the possible influence of epitaxial control, amorphous substrate (vitreous carbon) was selected to analyze the influence of only bath composition and deposition conditions. The vitreous carbon electrode was previously polished to a mirror finish by using alumina of different grades (3.75 and 1.87 μm) and ultrasonically cleaned for 2 min in water before each experiment. The counter-electrode was a platinum spiral. The reference electrode was Ag|AgCl|NaCl 1 M mounted in a Luggin capillary containing 0.2 M $NaClO_4$ solution.

Voltammetric experiments were carried out at 50 mV s^{-1}, scanning towards negative potentials. Only one cycle was run in each voltammetric experiment. Deposits were prepared potentiostatically under stirring conditions ($\omega = 100$ rpm) using a magnetic stirrer. Cobalt deposit nominal thicknesses were estimated from the deposition charge without taking into account the efficiency of the process.

Deposit structures were studied by means of X-ray powder diffraction (XRD), using a conventional Bragg-Brentano diffractometer Siemens D-500. The Cu Kα radiation ($\lambda = 1.5418$ Å) was selected by means of a diffracted beam curved graphite monochromator. X-Ray powder diffraction diagrams were obtained in the 10–130° 2θ range with a step range of 0.05° and a measuring time of 30 s per step. Morphology of deposits was observed using Hitachi S 2300 and Jeol JSM 840 scanning electron microscopes. A SQUID magnetometer was used to take the magnetic measurements at room temperature.

Table 1 Composition of the baths used to obtain cobalt coatings

Bath	Concentration (mol dm^{-3})				
	$Co(ClO_4)_2$	$NaClO_4$	Thiourea	Sodium gluconate	H_3BO_3
A	0.1	0.1	0	0	0
B	0.1	0.1	0.1	0	0
C	0.1	0.1	0	0.1	0
D	0.1	0.1	0	0	0.3
E	0.1	0.1	0.1	0.1	0.3

3 Results and discussion

3.1 Electrochemical study of the deposition process

Different electrolytic baths (A–E) (Table 1) were selected to prepare cobalt deposits. For each bath, cyclic voltammetry and potentiostatic techniques were used to give a phenomenological description of the deposition process. The potentiostatic technique was also used as the method to obtain cobalt deposits.

Cyclic voltammogram (Fig. 1, curve a) recorded from the additive-free bath (bath A), showed a clear reduction peak corresponding to cobalt electrodeposition. The reduction peak was related to a mass transfer controlled process because when the solution was stirred, the reduction current maintained a constant value. Reversing the scan at potentials corresponding to the onset of the reduction current, a clear current loop was observed corresponding to the nucleation and growth process of cobalt. Two oxidation peaks were observed during the anodic sweep. The peak at more positive potentials corresponds to cobalt oxidation. Meanwhile, the most negative peak is assigned to the oxidation of the hydrogen formed during the negative scan favoured by cobalt deposition. The charge associated with this peak decreased when the same voltammetric scan was performed under stirring conditions, suggesting that H_2 was removed from the electrode when stirring. A similar oxidation peak was detected in voltammetric curves recorded under stationary conditions for cobalt and cobalt alloy deposition processes in other baths at high cathodic limits [10, 11].

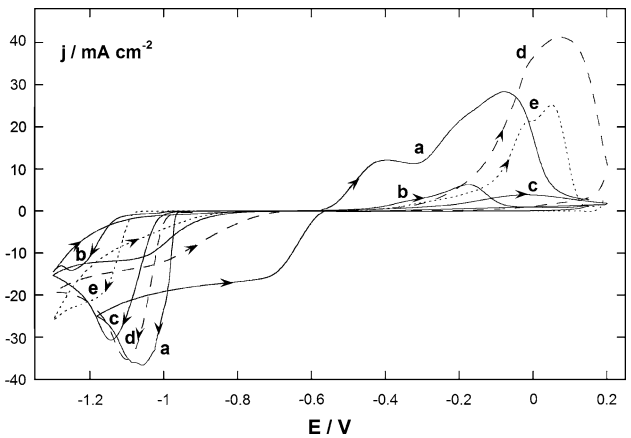

Fig. 1 Cyclic voltammograms of: (a) bath A, (b) bath B, (c) bath C, (d) bath D and (e) bath E

When different additives were added to the simplest bath, A, a shift in the onset of the cobalt deposition process as well as a decrease in the peak current, were observed in some cases. In all cases a nucleation loop was observed, reversing the scan at the onset of the deposition process. The presence of thiourea in the bath (bath B) (Fig. 1, curve b) caused not only an important delay in the onset of the cobalt deposition process but also a decrease in the current peak. Thiourea forms a complex with cobalt [12], and this Co-thiourea complex is chiefly responsible for the shift observed at the onset of the reduction process as well as the decrease observed in the peak current (as a consequence of a sharp decrease in the diffusion coefficient with respect to that of free cobalt ions). On the other hand, under these conditions no clear reduction peak was developed due to the close and simultaneous hydrogen evolution.

The addition of either sodium gluconate (bath C) (Fig. 1, curve c) or boric acid (bath D) (Fig. 1, curve d) had a lesser effect on the cobalt electrodeposition process than thiourea, although a clear shift of the onset of the deposition process as compared to the additive-free bath (bath A) was observed. With the presence of sodium gluconate, there was not only a delay in the cobalt reduction but also a decrease in the current peak. Two factors may explain the voltammetric change. On one hand, slight complexation of cobalt by sodium gluconate [12] shifts the reduction potential and decreases the peak current due to the 30% reduction in the diffusion coefficient. On the other hand, adsorption on the electrode may also contribute to the shift in reduction potential. Adsorption was considered because of the small oxidation charge recorded during cyclic voltammetry, suggesting that the high adsorption capacity of sodium gluconate on cobalt electrodes hinders cobalt oxidation. The small anodic charge was not attributed to passivation of cobalt films because no oxides were detected by either XRD or XPS [13]. When boric acid is present in the bath (bath D), only a delay in the onset of the reduction potential is observed. This delay is attributed to the adsorption of this species on the electrode because boric acid has no clear complexing capacity for cobalt ions.

The bath simultaneously containing thiourea, sodium gluconate and boric acid (bath E) showed an intermediate potential delay between those observed in thiourea and sodium gluconate or H_3BO_3 indicating that cobalt was slightly uncomplexed by thiourea (Fig. 1, curve e). Under these conditions no clear reduction peak was developed.

After selecting, from voltammetric experiments, the potential zone in which cobalt electrodeposition occurred in each bath, a potentiostatic study of cobalt deposition was performed.

Figure 2 shows the j–t transients recorded from the different baths tested. The j–t transient recorded from bath A at low overpotential showed (Fig. 2, curve a) an induction time corresponding to the formation of the first nuclei, a sharp current increase related to the growth of the deposit and a maximum subsequent current decay corresponding to the depletion of Co(II) near the electrode. As expected, by raising the overpotential, the induction time was minimised and the maximum appeared at lower deposition times (Fig. 2, curve b).

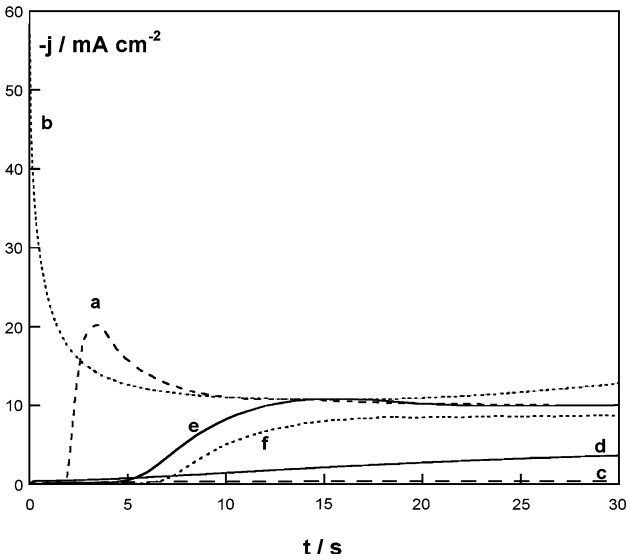

Fig. 2 j–t Transients of: (a) bath A at −840 mV, (b) bath A at −900 mV, (c) bath B at −1,000 mV, (d) bath C at −900 mV, (e) bath D at −900 mV and (f) bath E at −950 mV. Quiescent conditions

In the other baths (baths B–E), lower currents were detected at similar deposition potentials according to the shifts of the cobalt electrodeposition processes recorded during the voltammetric study. For bath B, high negative overpotentials needed to be applied to observe current (Fig. 2, curve c). In this bath, the recorded current values in the j–t transients were always lower than those recorded in the thiourea–free bath. This was due to the Co–thiourea complex formation and hence to the decrease in diffusion coefficient of the electroactive species as previously detected in voltammetric experiments.

The presence in the bath of either sodium gluconate (bath C) (Fig. 2, curve d) or boric acid (bath D) (Fig. 2, curve e) slowed down the cobalt deposition process but less than for thiourea. At −900 mV, the comparison between the recorded j–t transient from bath A (Fig. 2, curve b) and those from baths C and D (Fig. 2, curves d and e) showed that the addition of either sodium gluconate or boric acid slowed the process, with the former producing a more pronounced effect, according to the voltammetric results. When the three species were present in the bath (bath E), higher overpotential was needed to record similar currents than from baths C and D (Fig. 2, curve f).

3.2 Cobalt deposits preparation and characterization

Potentiostatic deposition of cobalt films was performed taking into account the results of the electrochemical study. Cobalt deposits between 0.5 and 5 μm (deposition charge between 1.6 and 16 C cm^{-2}) were prepared at moderate stirring conditions (100 rpm) to maintain the contribution of the Co(II) species to the electrode. A morphological study over a wide potential range was made. Structural and magnetic properties of cobalt electrodeposits prepared from the different baths at potentials corresponding to the onset of cobalt deposition were compared. From each bath, the properties of deposits of equal charge were compared.

3.2.1 Morphological analysis

The morphology of deposits prepared from baths A to E was studied. No significant modification in deposit morphology was observed as a function of deposition charge in any of the baths.

Cobalt deposits prepared from the additive-free bath (bath A) at different deposition potentials (from −870 mV to −1,150 mV) were metallic grey and presented nodular morphology (Fig. 3). As the potential became more negative a decrease in grain size was detected. This grain size decrease revealed the ease of nucleation over grain growth at high negative deposition potentials.

The presence of thiourea in the bath (bath B) induced the formation of black deposits. These deposits, even those obtained at low overpotentials, were characterized by nodular morphology with a great number of voids (Fig. 4) probably related to hydrogen evolution or hydroxide precipitation, which hinders compactness. The electrocatalytic

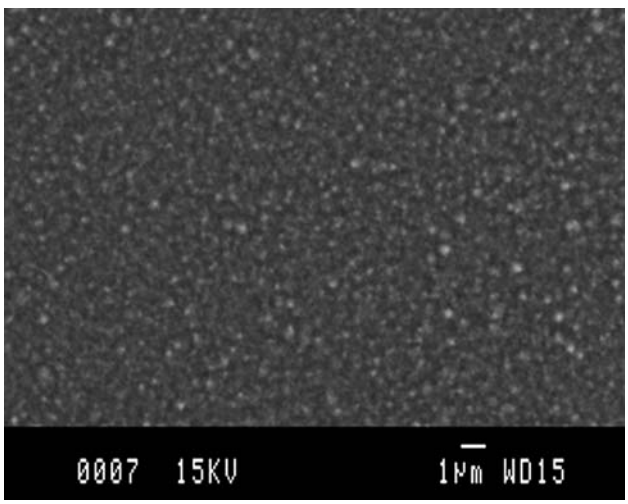

Fig. 3 Scanning electron micrograph of Co deposits of 0.5 μm prepared at −870 mV from bath A

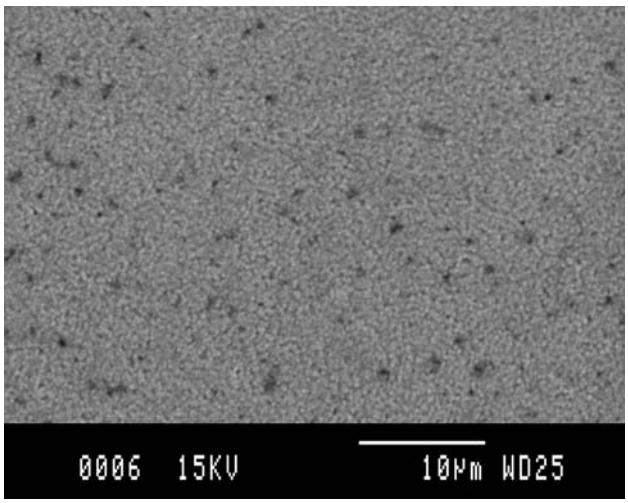

Fig. 4 Scanning electron micrograph of Co deposits of 0.5 μm prepared at −1,000 mV from bath B

behaviour of Co to hydrogen evolution may explain the high number of voids observed in the deposits prepared from this bath.

The addition of sodium gluconate or boric acid made it possible to obtain metallic grey cobalt deposits. When sodium gluconate was present (bath C) different morphologies were detected depending on the applied potential. At very low overpotentials well-separated, quasi-spherical grains were seen to grow at isolated locations over the first deposited layer with nodular morphology (Fig. 5a). A slightly higher overpotential was needed to obtain compact deposits, characterized by acicular morphology (Fig. 5b). The adsorption of gluconate during cobalt growth may be responsible for the change in deposit morphology. On the other hand, the presence of boric acid (bath D) made it possible to also obtain compact deposits with slightly faceted-grain morphology (Fig. 5c) in all conditions tested.

The simultaneous presence of boric acid and sodium gluconate in the bath containing thiourea (bath E) improved the deposit quality, showing coatings with nodular morphology (Fig. 6) but higher grain size than that observed in deposits obtained from bath A. Deposits obtained from this complex bath were crack-free and had high compactness throughout the entire range of potentials studied.

3.2.2 Crystal structure and magnetic properties

X-ray diffraction patterns and magnetic behaviour of cobalt deposits obtained from baths A to E of around 4 μm were studied The deposits were obtained at low applied potentials (from −870 mV for bath A to −1,000 mV for bath B; the potentials for the other baths were between −870 and −1,000 mV) in order to minimize the possible hydrogen reaction. The variation of these properties as a function of

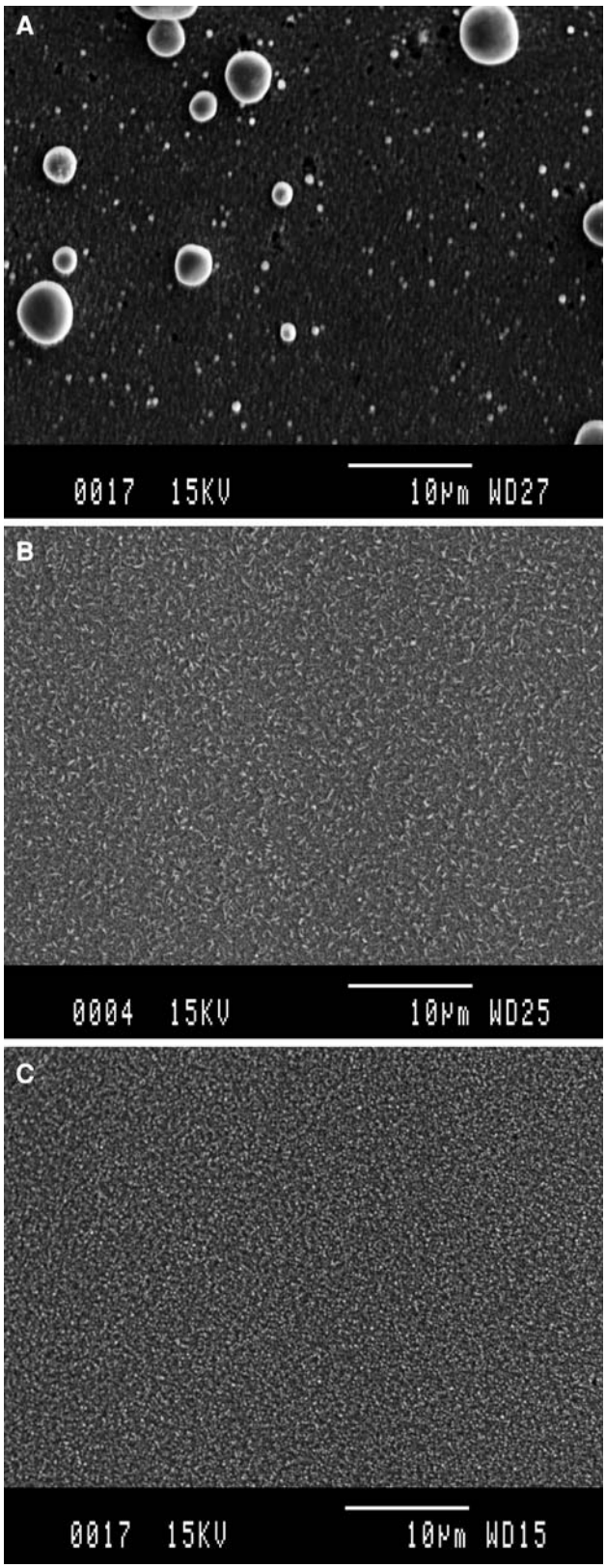

Fig. 5 Scanning electron micrographs of Co deposits of 0.5 μm prepared from (**a**) bath C at −800 mV, (**b**) bath C at −850 mV and (**c**) bath D at −850 mV

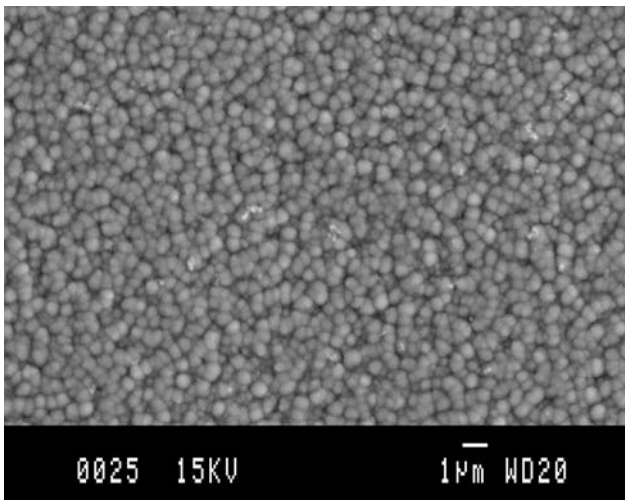

Fig. 6 Scanning electron micrograph of Co deposits of 0.5 μm prepared at −900 mV from bath E

bath composition was analysed. Cobalt deposits were removed from the vitreous carbon electrode and placed on a silicon monocrystalline substrate of low response for X-ray spectra recording.

The diffractograms of cobalt deposits prepared from the different baths, except bath B, showed narrow peaks as compared to the response of the substrate, revealing their crystalline nature. Figure 7a and b show the diffractograms of the crystalline deposits. The width of the diffraction peaks was greater than the instrumental peak linewidth, revealing the nanometric size of the crystallites. However, when cobalt deposits were obtained from bath B, the diffractogram showed practically the same response as the substrate (Fig. 7c), revealing the amorphous nature of this film.

Table 2 summarizes the information derived from the XRD patterns: structure, main planes and I/I_{max} ratio of the deposits studied. The X-ray diffractograms of the films obtained from baths A, C and D are characterized by showing a close-packed hexagonal structure (hcp) but different preferred orientation. Whereas cobalt samples obtained from baths A and D are textured with a (110) preferential orientation (but with a different peak intensity distribution), hcp cobalt phase from bath C grows with the (002) plane as preferred orientation. Positions of the peaks remained constant in all the spectra and equal to those tabulated [PDF#05-0727], implying the same lattice parameters. Due to the constancy of these parameters it could be suggested that the species are not incorporated within the lattice and that the adsorption of these species during electrodeposition is responsible for the change in the preferential orientation. Although the same structure was detected, the different orientation of the films as well as the different peak intensity distribution gave rise to

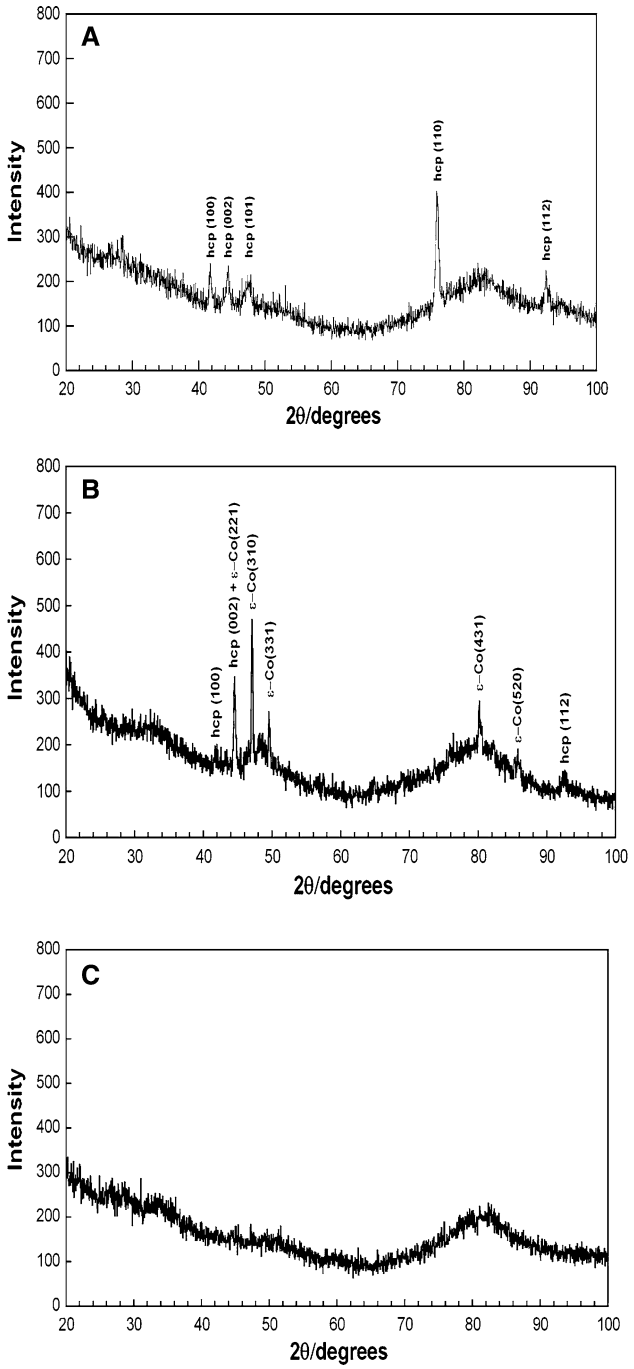

Fig. 7 XRD patterns of Co deposits of 4 μm obtained from: (**a**) bath A, (**b**) bath E and (**c**) bath B

different morphologies: nodular morphology (bath A), faceted-grain morphology (bath D) and acicular morphology (bath C).

On the other hand, when all the species were present in the solution (bath E) a primitive cubic structure (ε-Co), different from the usual hcp or fcc cobalt phases, was detected as the main phase. Coupled to this structure, some hcp phase can be observed. Also in this case, the different

Table 2 Structural properties of cobalt coatings

Bath	Structure	Planes	I/I_{max} (%)
A	hcp	(100)	37
		(002)	31
		(101)	22
		(110)	100
		(112)	31
B	Amorphous	–	–
C	hcp	(100)	36
		(002)	100
		(101)	44
		(110)	40
D	hcp	(100)	61
		(002)	16
		(101)	35
		(110)	100
		(112)	20
E	hcp + ε-Co (primitive cubic)	hcp (100)	17
		hcp (002) + ε-Co (221)	71
		ε-Co (310)	100
		ε-Co (331)	36
		ε-Co (431)	36
		ε-Co (520)	17
		hcp (112)	12

structure detected was associated with a different morphology: a nodular morphology with a higher grain size than that observed in films obtained from the simplest bath (bath A). The primitive cubic phase of cobalt (ε-Co) has been detected for cobalt nanoparticles synthesized by wet chemical synthetic routes [14, 15] or cobalt nanocrystals [16, 17] but not by electrochemical methods.

The average grain size was estimated from the full width at half maximum (FWHM) values of the diffraction peaks by using the Debye-Sherrer equation, neglecting the instrumental linewidth (which is acceptable for a nanocrystalline material) and the stress-induced line broadening. For the cobalt crystalline deposits prepared from the different baths tested, no significant differences were observed in the estimated grain size in the range 20–30 nm for all the films.

The magnetic behaviour of cobalt films was analysed by recording hysteresis loops. Figure 8 shows two representative magnetization-magnetic field dependences. A saturation magnetisation (M_s) of around 150–160 emu g^{-1} (that corresponds to the value for bulk cobalt) was obtained for all samples.

From the parallel and perpendicular hysteresis loops obtained with the SQUID, very different values of the saturation fields (H_s) were observed for parallel ($H_{s_\parallel}$) and perpendicular ($H_{s_\perp}$) fields for cobalt deposits showing hcp structure (deposits obtained from A, C and D baths)

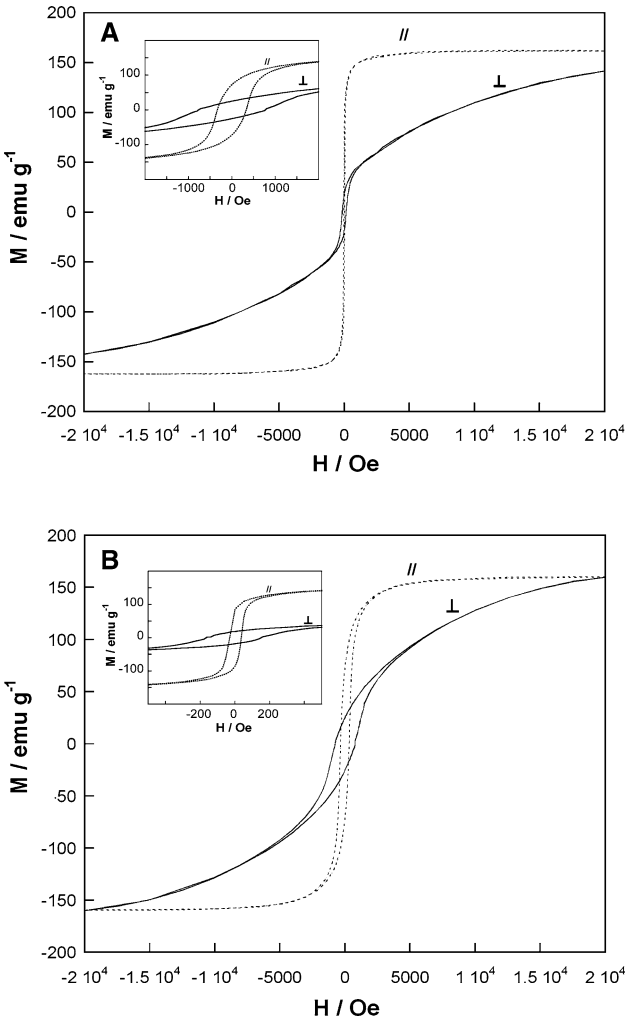

Fig. 8 Magnetisation versus magnetic field of Co deposits of 4 μm obtained from (**a**) bath A and (**b**) bath C

Table 3 Magnetic properties of cobalt coatings: Coercivity values (H_c), saturation fields (H_s), uniaxial anisotropy constant (K) and calculated angle of the resulting anisotropy with respect to the film normal (θ)

Bath	H_c (∥) (Oe)	H_c (⊥) (Oe)	H_s (∥) (Oe)	H_s (⊥) (Oe)	K (J cm^{-3})	θ (°)
A	31	149	11,000	40,000	2.36	55
B	15	25	–	–	–	–
C	344	767	15,000	32,000	2.07	45
D	86	183	12,000	40,000	2.43	54
E	117	100	13,000	15,000	0.21	5

(Fig. 8; Table 3), revealing the magnetic anisotropy of these films. An easier magnetization direction in the parallel-applied field was observed. The anisotropy was not parallel to the applied field. A high uniaxial anisotropy constant (K) and the angle of the resulting anisotropy with respect to the normal film (θ) were estimated for these deposits using the expressions [18]:

$$H_{s_{\parallel}} = 2K\cos^2\theta/M_s \quad (1)$$

and

$$H_{s_{\parallel}} + H_{s_{\perp}} = 4\pi M_s + 2K/M_s \quad (2)$$

The values of K were greater than that corresponding to pure hcp cobalt ($K = 0.45$ J cm^{-3}) [19] probably due to internal stress. A spontaneous orientation of the film parallel to the magnetic field confirmed the strong uniaxial anisotropy, in addition to the usual shape anisotropy expected for thin films [19].The calculated angle θ was 45–55° in the three cases.

Less difference between M–H loops with the magnetic field perpendicular or parallel to the film plane was observed for cobalt amorphous films prepared from bath B or cobalt ε-Co + hcp obtained from bath E, suggesting no significant magnetic anisotropy in these films. Regarding the unusual primitive cubic cobalt phase, the calculated value ($K = 0.21$ J cm^{-3}) is close to that found in the bibliography for nanocrystals with cubic ε-Co structure embedded in an amorphous carbon matrix [20]. A clearly different value of the calculated θ was obtained for these films. On the other hand, the value of K for amorphous cobalt cannot be calculated because of the lack of magnetic anisotropy associated to the short-range order.

Noticeable differences were also detected in coercivity values (H_c) for the cobalt films prepared in the different electrolytic baths (Table 3), both in the easy and the hard axis of magnetization. The highest coercivity observed was in cobalt films obtained from bath C and the lowest value was measured in the cobalt deposits obtained from bath B. Whereas cobalt deposits from baths A and D, with the hcp structure and the same preferred orientation, show similar H_c values, the cobalt deposits obtained from bath C, also with hcp structure, show a much higher value mainly associated to the change in the preferential orientation. A different value of coercivity was also observed for deposits prepared from complex bath E, associated with the structural change induced for the components of the bath. The lowest value of coercivity was detected in the amorphous films obtained from bath B. For these amorphous deposits, the lack of macroscopic magnetocrystalline anisotropy implies a relatively easy magnetization rotation. Furthermore the absence of microstructural discontinuities (grain boundaries or precipitates), on which magnetic domains can be pinned, makes magnetization by wall motion easy and, hence, coercive fields of a few oersteds are achieved.

4 Conclusions

Electrodeposition has been shown to be a suitable technique for obtaining cobalt films with tailored magnetic

properties, because the different species tested (boric acid, gluconate and thiourea) induced different structural properties and even amorphous nature in the deposits. Moreover, structural changes are reflected in the different morphologies observed.

The electrochemical study allowed us to detect the dependence of the cobalt electrodeposition process on bath composition. Coherent and uniform cobalt deposits were obtained from baths containing boric acid or gluconate. Although the presence of only thiourea did not favour the formation of uniform cobalt deposits the combination of thiourea with gluconate and boric acid made it possible to obtain coherent films in a wide range of potentials. The baths tested favoured the appearance of singular orientations with different types of magnetic behaviour. The use of these different species allowed us to modulate the magnetic response of the cobalt deposits.

Cobalt films obtained from baths A and D showed hcp structure with (110) as preferred orientation. The similar structural characteristics in both cases justify the similar coercivity values (around 150 Oe).

The highest value of H_c (around 380 Oe) was observed in cobalt coatings of hcp structure, (002) preferred orientation and acicular morphology obtained from bath C. The lowest H_c (around 15 Oe) was detected in cobalt films obtained from bath B due to the amorphous nature of these deposits.

A primitive cubic phase (ε-Co) was detected in cobalt obtained from the most complex bath (bath E), revealing that an unusual structure of cobalt films can be induced by the simultaneous presence of complexing agents and adsorbed species.

Depending on the bath composition, it was then possible to obtain cobalt electrodeposits with different magnetic properties. While the presence of thiourea induced the formation of soft magnetic films, sodium gluconate made it possible to obtain harder magnetic coatings. An intermediate behaviour was detected when all the species were present in the bath. Thus the possibility of developing new electrodeposition baths containing the species tested with the objective of preparing Co containing films with tailored magnetic properties is open.

Acknowledgements This paper was supported by contract MAT-2006-12913-C02-01 from the *Comisión Interministerial de Ciencia y Tecnología (CICYT)*. J. García-Torres also thanks the Departament d'Innovació, Universitats i Empresa of the Generalitat de Catalunya and Fons Social Europeu for financial support.

References

1. Higashi K, Fukushima H, Urkawa T, Adaniga T, Matsudo K (1990) J Electrochem Soc 137:3418
2. Osaka T (2000) Electrochim Acta 45:3311
3. Moina CA, de Oliveira-Versic L, Vazdar M (2004) Mater Lett 58:3518
4. Brückner W, Thomas J, Hertel R, Schäfer R, Schneider CM (2004) J Magn Magn Mater 283:82
5. Gómez E, Vallés E (2002) J Appl Electrochem 32:693
6. Cui CQ, Jiang SP, Tseung CC (1990) J Electrochem Soc 137:3418
7. Ankara S, Majan S (1980) J Electrochem Soc 127:283
8. Gómez E, García-Torres J, Vallés E (2007) Anal Chim Acta 602:187
9. Gómez E, García-Torres J, Vallés E (2008) J Electroanal Chem 615(2):213
10. Pellicer E, Gómez E, Vallés E (2006) Surf Coat Technol 201:2351
11. Gómez E, Pellicer E, Vallés E (2003) J Electroanal Chem 556:137
12. IUPAC Stability Constants Database (SC Database) version 5.16 (2001) Ed. Academic Software cop
13. García-Torres J, Gómez E, Alcobe X, Vallés E Surf Coat Technol (Submitted)
14. Sun S, Murray CB (1999) J Appl Phys 85:4325
15. Puentes VF, Krishnan KM, Alivasatos P (2001) Appl Phys Lett 78:2187
16. Nie X, Jiang JC, Meletis EI, Tung LD, Spinu L (2003) J Appl Phys 93:4750
17. Sun S, Murray CB (1999) J Appl Phys 85:4325
18. Xiao JQ, Chien CL, Gavrin A (1996) J Appl Phys 79:5309
19. Klavunde KJ (2001) Nanoscale materials in chemistry. Wiley-Interscience, New York
20. Nie X, Jiang JC, Meletis EI, Tung LD, Spinu L (2003) J Appl Phys 93:4750